THE BELL SYSTEM TECHNICAL JOURNAL
Vol. 57, No. 6, July–August 1978
Printed in U.S.A.

Atlanta Fiber System Experiment:

Planar Epitaxial Silicon Avalanche Photodiode

By H. MELCHIOR, A. R. HARTMAN, D. P. SCHINKE, and T. E. SEIDEL

(Manuscript received March 1, 1978)

A silicon avalanche photodiode (APD) has been developed for optical fiber communications systems. It has been optimized for optical wavelengths of 800 to 850 nm and exhibits a quantum efficiency greater than 90 percent. The APD operates between typical voltages of 100 and 400 V, exhibiting photocurrent gains of approximately 8 and 100, respectively, at those biases. The device has a short response time of ~1 ns and low excess noise characterized by an excess noise factor approximately 5 times the shot noise limit for operation at a photocurrent gain of 100. The APD has a four-layer n^+-p-π-p^+ structure and is fabricated on large-diameter epitaxial wafers using planar technology. Uniform avalanche gain, low dark currents, and good reliability are achieved through the use of (i) a diffused guard ring, (ii) a diffused channel stop, (iii) metal field plates, (iv) the removal of impurities in the surface oxides and the bulk of the APD, (v) passivation with silicon nitride and (vi) a processing sequence that maintains low dislocation density material.

I. INTRODUCTION

Solid-state photodetectors are particularly well suited to optical communications. The detectors, fabricated from semiconducting materials, are small, fast, highly sensitive and relatively inexpensive.[1] Two widely employed detectors are the PIN photodiode, which in reverse bias collects the photogenerated minority carriers, and the avalanche photodiode, which has a high field region that multiplies the photocurrent through the avalanche generation of additional electron-hole pairs.

The avalanche photodiode (APD) designed specifically for the FT3 optical communications system[2] will be described in this paper. At a bit

rate of 44.7 Mb/s, the APD allows an increase in system sensitivity by approximately 15 dB over the same receiver with a PIN detector.[3] This improvement is possible because the shot noise in the photocurrent of the PIN diode is much smaller than the equivalent input noise of a receiver amplifier having sufficient bandwidth to carry the 45 Mb/s signal.[4] The gain in the APD increases the signal intensity and system sensitivity until the noise in the multiplied current is comparable to the noise of the amplifier. The avalanche photodiode is not, however, an ideal multiplier. It adds a substantial amount of noise because of fluctuations in the avalanche gain. The excess noise depends on the device structure and the electron and hole ionization rates of the material chosen for the detector.[5] The avalanche photodiode for the FT3 application was designed to minimize excess noise and maximize the quantum efficiency without compromising manufacturability or reliability.

In Section II, the design and operation of the APD are described. The fabrication is outlined in Section III, and the optical and electrical characteristics are given in Section IV.

II. DESIGN AND OPERATION

Since the wavelengths of the GaAlAs double heterostructure laser employed in the FT3 system are 800 to 850 nm, the choice of silicon as the detector material is the obvious one. These wavelengths require photocarrier collection lengths of 20 to 50 μm, which lie well within the range of achievable space charge layer widths in lightly doped material.

For lowest noise, McIntyre[5] has shown that in silicon the avalanche should be initiated by pure electron injection into a relatively wide gain region. This results from the high ratio of the electron-to-hole ionization rates favoring electron multiplication by a factor of 10 to 50 for the electric fields of importance.[6] The avalanche photodiodes combining the highest efficiency and speed (in the 800- to 900-nm wavelength range) with high uniform current gains and low excess noise are then constructed from silicon as n^+-p-π-p^+ structures and operated at high reverse bias voltages with fully depleted p-π regions. In these devices, incident light in the 800- to 900-nm range is mainly absorbed in the π region. From the π region, the photogenerated electrons drift into the n^+-p high field region where they undergo avalanche carrier multiplication. This device structure is referred to as a reach-through structure.[7-9] To achieve the lowest noise operation associated with pure electron injection, the light should be incident through the p^+ contact and fully absorbed in the π region. These APDs must be bulk devices thinned to 50 to 100 μm before metallization[8] or epitaxial devices having n^+ substrates and two sequential epitaxial p and π layers.[10]

A device construction more amenable to fabrication on large-diameter

silicon wafers with good control of the doping profile utilizes π-type epitaxial silicon on p^+ substrates and forms the n^+-p-π-p^+ structure through ion implantation and diffusion. This construction, as shown in cross section in Fig. 1, dictates that the light be incident through the n^+ contact on the epitaxial surface of the device. The noise penalty brought about by the resultant generation and injection of electrons and holes into the high-gain region is minimized by tailoring the field profile. With a shallow n^+ and a deeply diffused p-type region, the electric field profile in the p-region is essentially triangular with the maximum field at the n^+-p junction. Employing the noise analysis of Webb et al.,[5] the triangular field profile results in lower noise operation for front-illuminated APDs, when compared to a rectangular field profile. The electrons injected from the π into the p-region encounter a low field and the holes generated within and in front of the gain region encounter a large field, both of which are shown by this analysis to be beneficial for low-noise carrier multiplication.[11]

While the noise of the gain process for front-illuminated epitaxial devices is somewhat larger than for back-illuminated bulk devices, the difference has only a small influence of approximately 1 dB on the overall receiver sensitivity. Device construction from epitaxial silicon makes fabrication with large-diameter wafers possible and avoids thinning and handling bulk wafers.

Referring to the cross section of the device, the epitaxial π region is typically 40 μm thick, has a resistivity in excess of 300 Ω-cm, and is grown

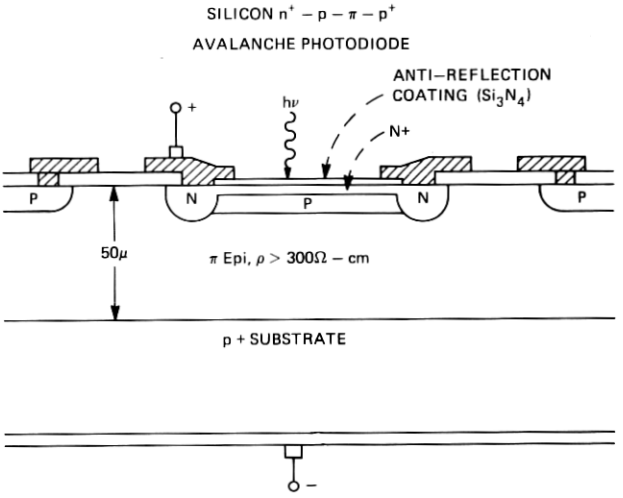

Fig. 1 — Cross-sectional view of epitaxial silicon n^+-p-π-p^+ avalanche photodiode made for illumination through the n^+ contact layer. Diameter of the light-sensitive high-gain region is 100 μm.

on dislocation-free boron-doped substrates. The light doping of the π region is required to minimize the voltage required to deplete the entire region between the n^+ contact and the p^+ substrate. The p^+ channel stop diffusion surrounding the device cuts off surface inversion channels, limits the lateral spreading of the depletion region, and ensures that the depletion region will not extend to surface areas beyond the immediate perimeter of the device. The doping in the p-control charge region is determined by a boron ion implantation and subsequent drive-in. Deeper drive-in produces lower excess noise but increases the operating voltage. The n^+ contact under the optical window is made very shallow to minimize both the carrier recombination and the hole injection from the n^+ region to the p-region, which would increase the noise of the device. To avoid the low breakdown voltage associated with the small radius of curvature of the shallow n^+-π junction, an n guard ring is diffused around the perimeter of the junction. This guard ring also reduces constraints on the metal contact by providing a deep junction under the contact windows. The device is passivated over the exposed π region with SiO_2 and Si_3N_4 layers. Over the optical window, Si_3N_4 is deposited to a controlled thickness as an antireflection coating for normally incident radiation.

The metal contacts are arranged to overlap the metallurgical n-π and π-p junctions. These field plates prevent the buildup of charge within and at the surface of the SiO_2 and Si_3N_4 layers near the edges of the junctions. If charges on the surface of the dielectric were permitted to build up there, they could induce sufficiently large electric fields to cause bursts of avalanche and zener breakdown currents.[12] High levels of surface charge concentrations would ultimately lead to increased leakage currents and reduced breakdown voltages. The field plates also increase the breakdown voltage at the perimeter of the n-π junction by effectively increasing the radius of curvature of the guard ring diffusion.[13–15] The avalanche breakdown of the APD is then a bulk rather than surface effect because of the additional charge in the p-region. Similarly, the region of high multiplication lies within the optical window and has a diameter of $\sim$100 μm.

The planar epitaxial n^+-p-π-p^+ avalanche photodiode described above provides both high reliability and processing capability in large diameter silicon wafers. Similar epitaxial structures are achieving attention, as indicated in several recent publications.[3,10,16–19]

III. FABRICATION

The actual device fabrication begins with the growth on p^+ substrates of (>300 Ω-cm p-type) 50-μm thick epitaxial material. The structure of Fig. 1 is formed by first diffusing the n-type guard ring and p-type channel stop. A carefully controlled boron dose is then implanted and

diffused into the center region of the APD. A heavily doped phosphorus layer is diffused into the back of the wafer to getter deep level impurities in the silicon. This gettering substantially reduces the dark currents. A shallow n^+ (phosphorus) contact is deposited and the time of its drive-in diffusion is adjusted to control the current gain-voltage characteristics of the device. The wafers are annealed in an HCl ambient to reduce the mobile ion content of the surface oxide, and Si_3N_4 is deposited to passivate the structure. The Si_3N_4 is impervious to ionic contamination such as Na^+.

The n^+ diffused layers are removed from the back of the wafer, and an ohmic contact is formed by ion implantation of boron. At this point, the wafer is approximately 450 μm thick and has good mechanical strength. The front surface metallization is Ti-Pt-Au formed over sintered PtSi, and the back metal is Ti-Au.

PIN photodetectors are obtained with this fabrication sequence by omitting the boron ion implantation. Like the APDs, the PIN detectors have low leakage and capacitance and excellent reliability.

IV. CHARACTERISTICS

A relatively large number of optical and electrical characteristics contribute significantly to the performance of the avalanche photodiode. The characteristics of the n^+-p-π-p^+ APD that are of interest in the FT3 application are:

(*i*) Quantum efficiency.
(*ii*) Current gain-voltage characteristics.
(*iii*) Dynamic range.
(*iv*) Temperature and wavelength dependence of the gain-voltage characteristics.
(*v*) Uniformity of the gain under the optical window.
(*vi*) Excess noise as a function of wavelength and nominal gain.
(*vii*) Speed of response.
(*viii*) Capacitance.
(*ix*) Temperature dependence of the dark current.
(*x*) Reliability for 300-V operation.

The subject of system performance is treated in other papers in this volume.

4.1 Quantum efficiency

Consider first the quantum efficiency of the front-illuminated structure for normally incident radiation. The spectral response characteristics of Fig. 2 show the quantum efficiency of these avalanche photodiodes to be greater than 90 percent over the wavelength range from 680 to 860 nm. The accuracy of the measurements is $\sim\pm 5$ percent.

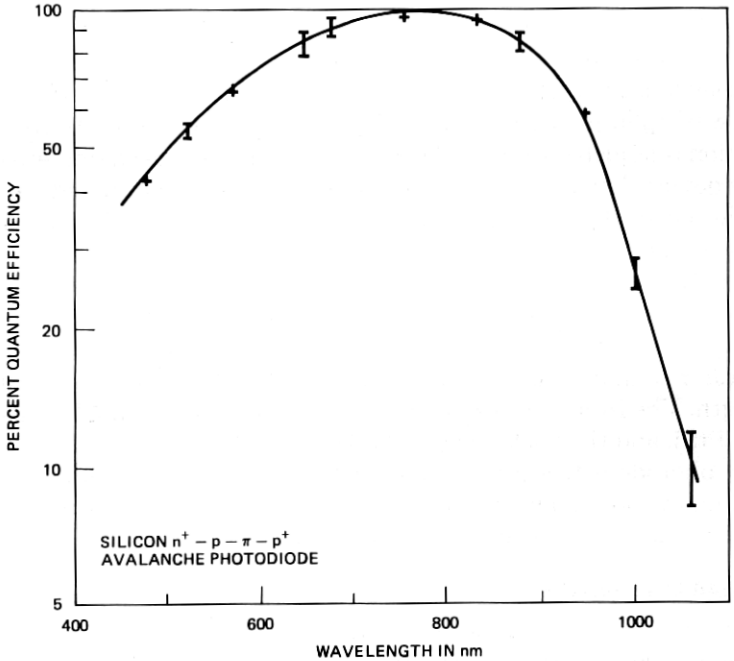

Fig. 2 — Spectral response curve of silicon n^+-p-π-p^+ avalanche photodiode with 40-μm wide π-type carrier collection region and SiO_2-Si_3N_4 antireflection coating.

The antireflection coating keeps the surface reflection to less than ~3 percent at 800 nm. Recombination in the thin n^+ contact and at the surface becomes substantial for wavelengths less than 600 nm. The response drops rapidly beyond 900 nm as the radiation penetrates deeply into the p^+ substrate.

4.2 Gain-voltage characteristics and dynamic range

Typical gain-voltage characteristics for different temperatures and with excitation at 825 nm are shown in Fig. 3. The operating bias range of these avalanche photodiodes extends from the onset of current gain at 60 V and complete sweepout around 100 V to avalanche breakdown at 250 to 400 V. At sweepout, the current gains (M) are between 5 and 10, and before breakdown they increase to values of several hundred.

In the FT3 system, the bias on the APD is decreased to reduce the gain for high levels of radiation. This current gain control adds to the dynamic range of the receiver. For the APD of Fig. 3, the dynamic range is given by the ratio of the maximum gain (M = 80 in the FT3 system) to the minimum gain ($M \simeq 6.5$ at 150 V bias), which is 11 dB of optical power. The minimum bias is determined by the speed of response requirements discussed in Section 4.5.

To preserve the dynamic range in the APD, the control charge doping was precisely adjusted to obtain the above characteristics. It is well

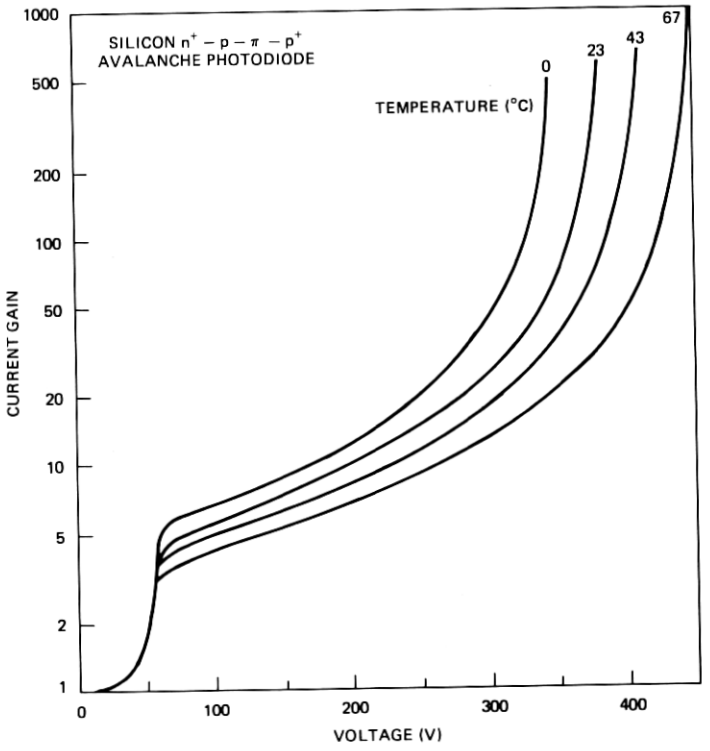

Fig. 3 — Current gain-voltage characteristic of silicon n^+-p-π-p^+ avalanche photodiode at different temperatures measured with excitation at 825 nm.

known that the breakdown voltage of n^+-p-π-p^+ structures are very sensitive to the charge of the p region.[20] A small increase of approximately 10 percent in the p region doping reduces the breakdown voltage by more than 100 V, but simultaneously increases the gain at the minimum bias. Lower voltage APDs are then characterized by lower dynamic range. For the front-illuminated APD with high resistivity epitaxy, the operating voltage range could be reduced from 150 V minimum–400 V maximum to 120 V minimum–200 V maximum (23°C), where the only engineering trade-off would be a reduction in the dynamic range from 12:1 (11 dB) to 4:1 (6 dB of optical power).

The gain-voltage characteristics show a pronounced dependence on temperature. As can be seen from Fig. 3, a bias voltage change of 1.4 V/°C is needed to keep the gain constant as a function of temperature. In addition, the gain-voltage characteristics show some dependence on wavelength of excitation, especially at short wavelengths, as shown in Fig. 4. The decrease in gain throughout the operating bias range at short wavelengths is due to mixed initiation of the avalanche by electrons and holes when most of the light is absorbed in the n^+-p region close to the silicon surface. The ionization coefficient for holes is smaller than that for electrons causing a reduction in the total current gain.

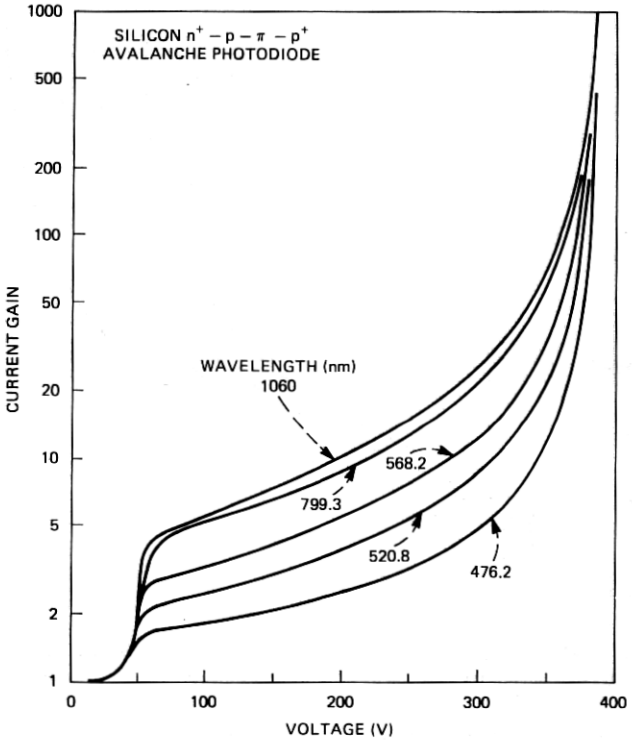

Fig. 4 — Current gain-voltage characteristics of silicon n^+-p-π-p^+ avalanche photodiode at room temperature for different wavelengths of optical excitation.

4.3 Current gain uniformity

The current gain uniformity is extremely important for the noise performance of the APD. Nonuniformities arise from two primary sources—crystalline defects and doping density fluctuations in the p-region.

Certain defects lead to premature breakdown spots or microplasmas. At their onset, the microplasmas generate irregularly fluctuating spikes of current that render the detectors useless for weak light signals. Through proper measures such as the choice of low dislocation materials and processing that does not introduce additional defects, the number of devices with disturbing microplasmas can be kept small.

All avalanche photodiodes exhibit high noise at the onset of bulk breakdown.[21,22] The breakdown noise is first observed as current pulses or spikes. In good devices, the breakdown noise threshold is substantially above the voltage for an average optical gain of 100, typically by 20 V. As the device is operated at higher gains, the regions of locally higher electric field develop a rapidly increasing tendency to support very large multiplication. Equivalently, the tail of the probability distribution extends rapidly to higher multiplications. A finite probability develops

that a single incident electron will produce a very large number of secondaries (i.e., 1000 to 10,000 carriers). The voltage onset of the avalanche noise is then believed to depend on the region of highest electric field in the APD.

A second source of electric field enhancement, after crystalline defects, is local fluctuations in the doping of the p region. When operating at an optical gain of 100, the APD will experience approximately 10 percent increase in gain for a doping fluctuation of 0.1 percent. The importance of the uniformity of the ion implantation for the p region cannot be overstated.

In the APD fabricated in this work, the avalanche carrier multiplication is quite uniform over the center part of the light-sensitive area of the diodes. This can be seen from Fig. 5, where the current gain as a function of position of the photoexcitation is shown for different bias voltages. At a maximum gain of 100, the gain is uniform within ±5 percent over a diameter of 75 μm and ±10 percent over a diameter of 90 μm.

4.4 Excess multiplication noise

The multiplication process in the avalanche photodiode increases the noise in the output current beyond the multiplied shot noise of the photocurrent. The source of the excess noise lies in the fluctuations in the avalanche process. The incident electrons are accelerated by the high

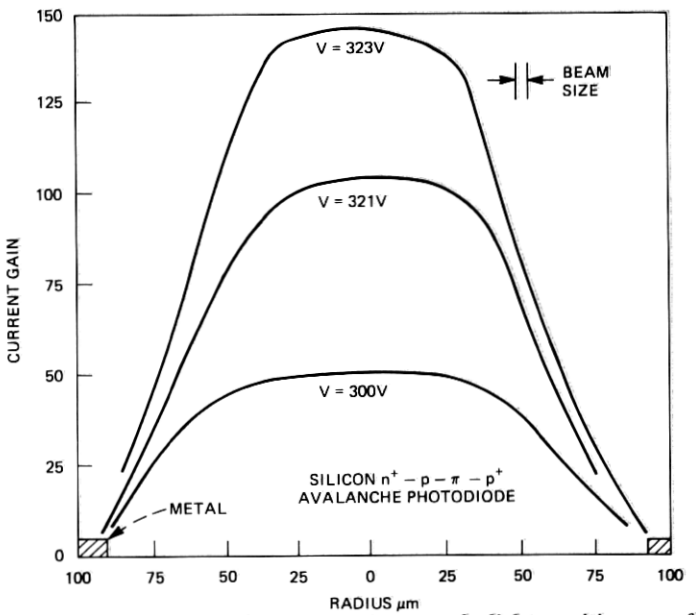

Fig. 5 — Spatial variation of the current gain across the light-sensitive area of an avalanche photodiode at different bias voltages. Measurements were done by scanning with a 3-μm light spot at 799.3 nm.

electric field and at the same time experience various inelastic scattering processes. When they achieve sufficient energy above the band gap, they can generate secondary electron-hole pairs. These charge carriers in turn gain sufficient energy to create additional electron-hole pairs. An ideal multiplier would provide exactly the same number of secondary electrons for each incident electron. In practice, the random nature of the scattering processes produces a broad distribution of multiplication factors. The current gain M of the APD is the average of the distribution of the multiplication factors. This statistical variation in the multiplication process increases the noise fluctuations of the output current.

A measure of the excess noise is given in the equation below, where the excess noise factor,

$$F(M) = \frac{\langle i_m^2 \rangle}{\langle i_{ph}^2 \rangle \times M^2}, \tag{1}$$

is defined as the measured mean-square noise current $\langle i_m^2 \rangle$ at the output of the avalanche photodiode divided by the product of the mean square noise $\langle i_{ph}^2 \rangle$ of the primary photocurrent and the square of the average gain M. Equivalently, the noise spectral density of the APD current is written as

$$\frac{d}{df} \langle i^2 \rangle = 2q \langle i_{ph} \rangle M^2 F(M). \tag{2}$$

The noise factor increases with gain reflecting a broadened distribution of multiplication factors. The development of a long tail in the distribution toward high multiplication factors at high electric fields was discussed in the previous section in connection with breakdown noise. The detailed dependence of $F(M)$ on M determines the optimum avalanche gain to be used with a given receiver front end and ultimately the optimum sensitivity of the receiver. The quantity $F(M)$ is often approximated by the relation $F(M) = M^X$, but a more exact expression, and one which is equally tractable mathematically, is[5]

$$F(M) = M\left[1 - (1-k)\left(\frac{M-1}{M}\right)^2\right] \tag{3}$$

or

$$F(M) = 2(1-k) + kM, \; M \gg 1. \tag{4}$$

where k is the effective ratio of the ionization coefficients of holes and electrons, suitably averaged over the high field region where avalanche occurs. The value of k depends upon the detailed electric field profile within the avalanche region and also upon the extent to which the avalanche is initiated by holes.

Shown in Fig. 6 is the excess noise factor of an APD as a function of

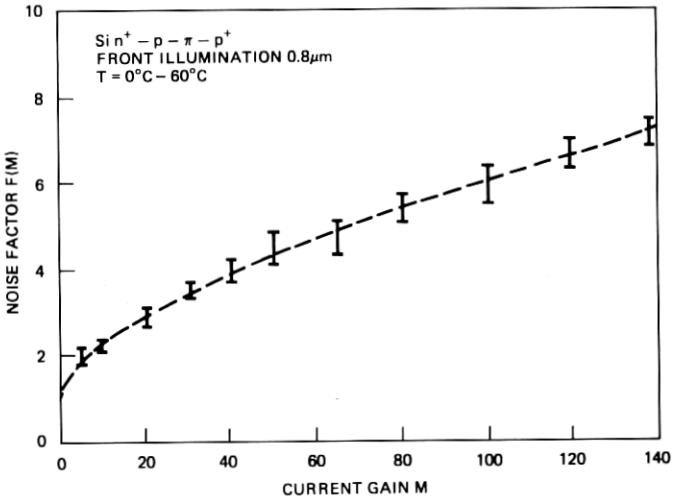

Fig. 6 — Noise factor $F(M)$ as a function of average current gain M for silicon n^+-p-π-p^+ avalanche photodiode at 800 nm. The measurement bars give an indication of the noise spread measured on devices made from different wafers.

gain. The measurement was done at room temperature; however, the excess noise factor is quite independent of temperature, at least over the 0° to 60°C range investigated. The excess noise at an average gain of 100 for excitation at 800 nm is only a factor of 5 to 6 higher than the shot noise limit of an ideal multiplier. This noise factor compares favorably with the noise factor of $F(M = 100)$ of 3 to 5 measured for the best bulk n^+-p-π-p^+ devices with illumination through the p^+ contact and pure electron initiation of the avalanche.[10] The value of k extracted from Fig. 6 at 800 nm is ~0.04.

Lower excess noise and k values are obtained for small increases in the width of the high field region. An extension of the multiplication region allows lower electric fields where the ratio of hole-to-electron ionization coefficients becomes even smaller.[8] However, the knee of the current gain-voltage characteristic (at 60 V in Fig. 3) corresponding to the depletion voltage of the p region moves to higher voltages increasing the voltage requirements for the APD. Additionally, for front-illuminated devices, wider p regions cause a larger fraction of the multiplication to be initiated by holes. For wide p regions, this effect determines the noise of the APD. Consequently, an optimum doping profile exists for the desired wavelength range. As discussed in Section II, the front-illuminated devices show lower noise for a triangular rather than a square electric field profile, where the initiating electrons first encounter a low electric field. To the first order, the electric field of the p region is essentially triangular because of the doping profile after drive-in.

Noise factor measurements on another APD with excitation at different wavelengths are shown in Fig. 7. While the lowest noise, $F(M = 100) =$

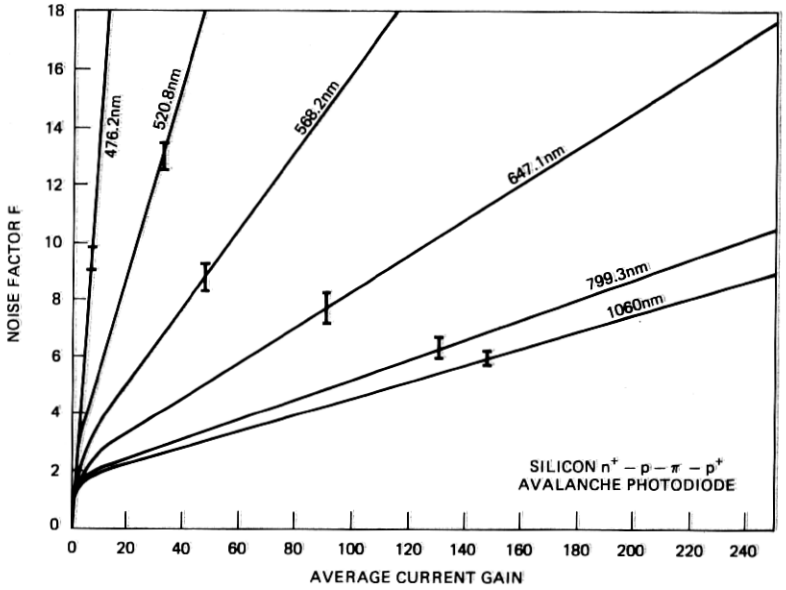

Fig. 7 — Noise factor $F(M)$ as a function of average current gain for optical excitation at different wavelengths.

4, is observed for excitation at long wavelengths at 1060 nm, the noise at 799 nm is not significantly higher, $F(100) \sim 5$. Actually, the diodes are quite low in excess noise even for mixed injection at 647 nm.

The overall penalty in optical sensitivity at $\lambda = 825$ nm incurred by the mixed injection of holes and electrons was $\lesssim 1$ dB of optical power. The ability to fabricate this device structure with a planar, high-voltage process is judged to outweigh the loss of 1 dB in sensitivity.

4.5 Response time and capacitance

To gain a measure of the speed of response, the duration of the multiplied output current pulses was investigated as a function of bias voltage for excitation with short laser spikes of 220 ps duration from a GaAlAs laser at 838 nm. The output pulses are quite symmetric in their rise and fall times without any tails at the end of the pulses. As depicted in Fig. 8, the duration of the output pulses at full depletion above 100 V is at most a few nanoseconds. At high bias voltages, where the holes drift with almost saturation-limited velocity through the π region, the pulse duration at 50 percent amplitude is less than 1 ns. At bias voltages less than 100 V, the pulse response becomes slower due to lower drift velocities and carrier diffusion within the undepleted π region.

The FT3 application requires a pulse width of 20 ns. To minimize jitter, the rise and fall times of the APD should be on the order of 1.0 to 2.0 ns. This requirement sets the minimum bias voltage at 150 V.

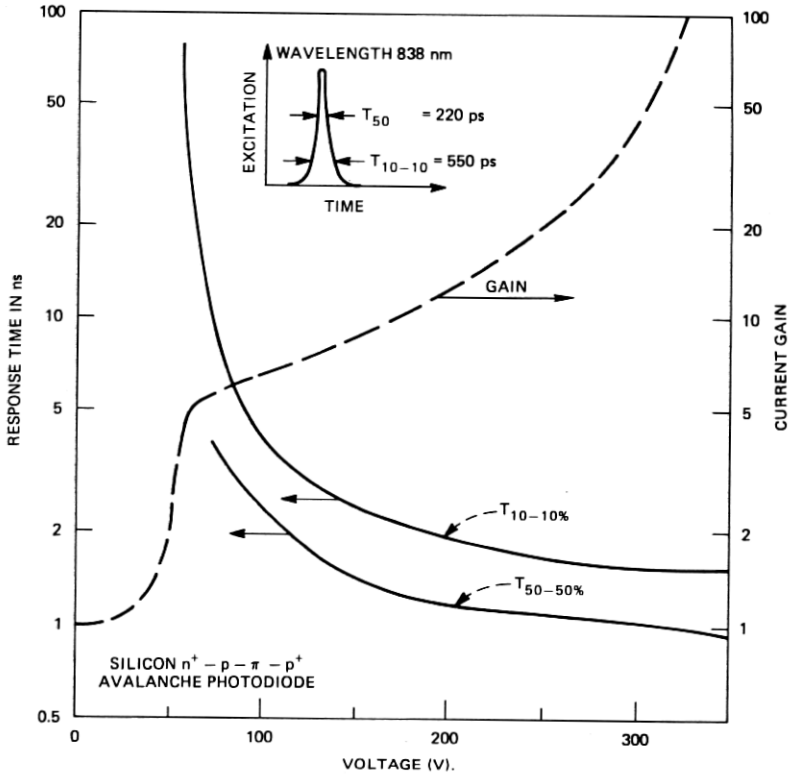

Fig. 8 — Response time and gain of multiplied photocurrent as a function of bias voltage for a silicon n^+-p-π-p^+ avalanche photodiode excited with pulses from a GaAlAs laser at 838 nm. The insert shows the shape and duration of the laser spikes as measured with a fast germanium photodiode.

Over the range of operating voltages, the capacitance of the avalanche photodiode is nearly independent of voltage. For a 40-μm π region, the capacitance is ~0.3 pF. The capacitance-voltage characteristic at lower voltages is given in Fig. 9. The gradual drop in capacitance between 0 and 50 V reflects the movement of the depletion layer through the p region. The rapid drop around 55 V corresponds to the movement of the depletion layer into the π region. The APD reaches full sweepout at ~85 V bias.

4.6 Leakage currents

Leakage or dark currents in the avalanche photodiode can be generated in the bulk of the depleted region due to thermal generation of carriers, or they can originate at the surface and bulk terminations of the space charge regions. The major part of the leakage of a typical APD is collected at the perimeter in a low field portion of the junction. These currents simply create a small offset that is not of importance to the

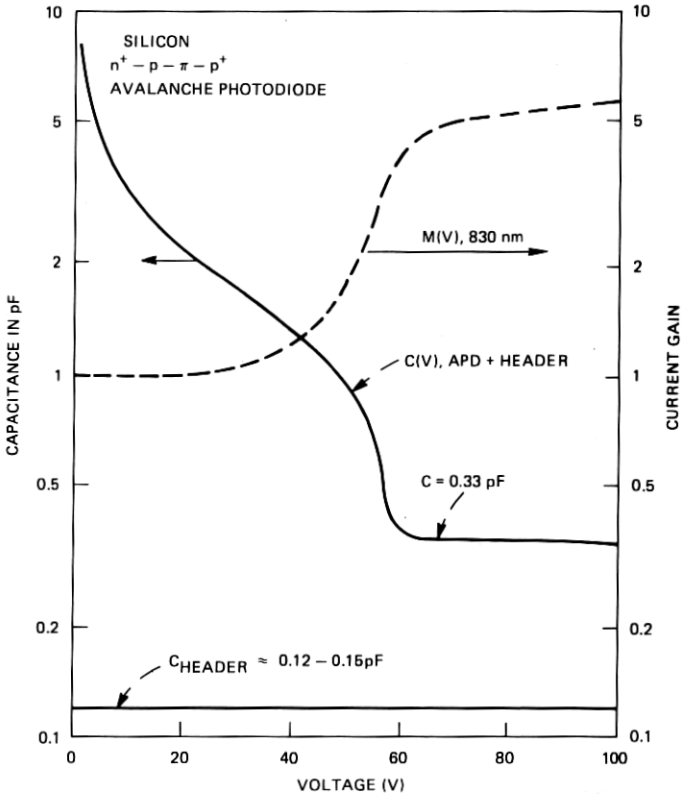

Fig. 9 — Capacitance and gain of an avalanche photodiode on a header as a function of bias voltage. From the difference between the total capacitance of the device and header and the capacitance of the header, it can be inferred that the capacitance of the device chip is between 0.2 and 0.3 pF at full depletion.

optical repeater. The leakage current collected in the high field portion of the junction is a potential source of noise since it experiences 80-fold multiplication in the APD. If the leakage current that is to be multiplied approaches the photocurrent induced by the laser in its off state, the noise of the APD would be increased. The smallest laser off-state photocurrents before multiplication fall between 10^{-10} and 10^{-9} A. By comparison, the leakage current to be multiplied is less than 10^{-12} A (at 23°C), and is negligible over the full temperature range of 0 to 60°C. Low leakage is achieved in these devices through the use of low dislocation materials, processes that avoid defect formation, and a back surface phosphorus diffusion gettering to eliminate fast-diffusing, deep-level impurities.

In Fig. 10, the dark current of a well-gettered APD with a 100-μm diameter active region is plotted as a function of reciprocal temperature. The dark current around room temperature is due to carrier generation

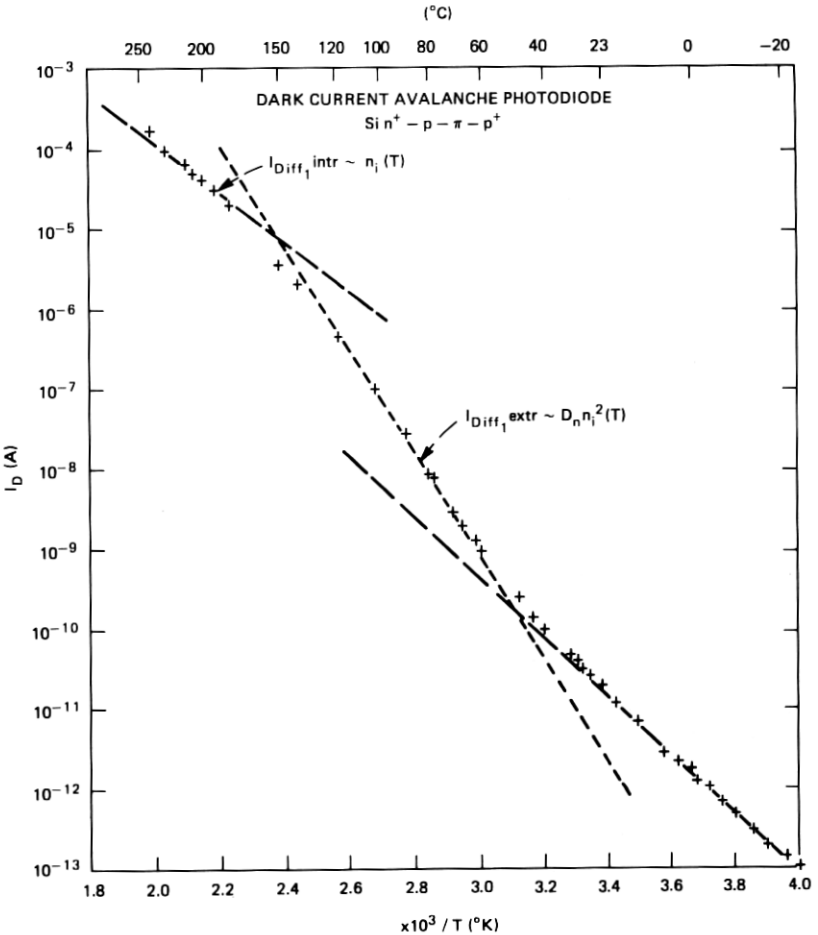

Fig. 10 — A plot of dark current as a function of reciprocal temperature for an avalanche photodiode with a 100 μm diameter high gain region and an overall diameter of 360 μm of fully depleted π region (40 μm thick).

from impurity centers with energy levels close to the middle of the bandgap. From the temperature dependence of the current between −20° and +40°C, the thermal activation energy for the carrier generation in these well-gettered devices is estimated to be 0.66 to 0.69 eV.

At higher temperatures between 40 and 150°C, the dark current increases with temperature in proportion to the square of the intrinsic carrier density as

$$n_i^2(T)D_n(T), \tag{5}$$

where $D_n(T)$ is the temperature-dependent diffusion constant of the electrons. Based on numerical estimates and measurements on devices of different diameters, it is suggested that this dark current component

is due to the diffusion of electrons out of the undepleted high resistivity π-type sidewalls of the device.

For temperatures in excess of 150°C, the intrinsic carrier concentration exceeds the doping in the π region. The leakage resulting from electron diffusion out of the APD's perimeter then increases in proportion to the intrinsic carrier concentration.[23]

4.7 Reliability

The avalanche photodiodes are reliable, having mean times to failure in excess of 10^3 hours at 200°C and 300-V bias in hermetic packages. Assuming an activation energy of 0.7 eV, which is estimated from the accelerated aging of several groups at different temperatures, the mean time to failure is in excess of 10^7 hrs at room temperature. This reliability results from the silicon nitride passivation, the gettering of mobile ions, and the use of field plates as discussed in Section II. Failures occur in devices without field plates because of surface charge accumulation over doped regions of the device. The surface charge induces high electric fields which reduce the breakdown voltage or produce breakdown noise.

V. SUMMARY

Front-illuminated, epitaxial silicon avalanche photodiodes having an n^+-p-π-p^+ structure are well suited to the detection of 800- to 900-nm radiation in fiber waveguide systems. The APD-developed for the FT3 system is a state-of-the-art device providing high quantum efficiency, ~1-ns response times, and low excess noise and dark currents. The APD allows ~15-dB improvement in receiver sensitivity, when compared to a nonavalanching photodiode. Its fabrication as a planar device on large-diameter, high-resistivity epitaxial wafers provides substantial improvements in manufacturability and reliability.

VI. ACKNOWLEDGMENTS

We are greatly indebted to R. P. Deysher and R. G. McMahon of Western Electric for the development and fabrication of the high-resistivity epitaxial material and to R. E. Carey and R. S. D'Angelo who contributed to the process development. Many helpful discussions with G. A. Rozgonyi, R. A. Moline, R. Edwards, R. G. Smith, A. U. MacRae, and M. DiDomenico are also acknowledged.

REFERENCES

1. H. Melchior, Physics Today, *30* (1977), p. 32.
2. J. S. Cook, J. H. Mullins, and M. I. Schwartz, paper presented at Conference on Lasers and Electro-optical Systems, San Diego, Calif. (1976), p.25.
3. H. Melchior and A. R. Hartman, Technical Digest of the International Meeting on Electron Devices (Wash., D.C.), IEEE, New York (1976), p. 412.

4. S. D. Personick, *Fundamentals of Optical Fiber Communications,* New York: Academic Press, 1976, p. 155.
5. R. J. McIntyre, IEEE Trans Electron Dev., *ED-13* (1966), p. 164.
6. C. A. Lee, R. A. Logan, J. J. Kleimack, and W. Wiegman, Phys. Rev., *A134* (1964), p. 716.
7. H. Ruegg, IEEE Trans. Electron Dev., *14* (1967), p. 239.
8. P. P. Webb, R. J. McIntyre, and J. Conradi, RCA Rev., *35* (1974), p. 234.
9. J. Conradi and P. P. Webb, IEEE Trans. Electron Dev. *22* (1975), p. 1062.
10. T. Kaneda, H. Matsumoto, T. Sakurai, and T. Yamaoka, J. Appl. Phys., *47* (1976), p. 1605.
11. H. Melchior, D. P. Schinke, and A. R. Hartman, unpublished work.
12. S. R. Hofstein and G. Warfield, IEEE Trans. Electron Dev., *ED-12* (1965), p. 66.
13. S. M. Sze and G. Gibbons, Solid State Electron., *9* (1966), p. 831.
14. D. S. Zoroglu and L. E. Clark, IEEE Trans. Electron Dev., *ED-19* (1972), p. 4.
15. L. E. Clark and D. S. Zoroglu, Solid State Electron., *15* (1972), p. 653.
16. H. Kanbe, T. Kimura, Y. Mizushima, and K. Kajiyama, IEEE Trans. Electron Dev., *ED-25* (1976), p. 1337.
17. T. Kaneda, H. Matsumuoto, T. Sakurai, and T. Yamaoka, J. Appl. Phys. *99* (1976), p. 1151.
18. S. Takamiy, A. Kondo, and K. Shirahata, Meeting of the Group on Semiconductors and Semiconductor Devices, Inst. of Elect. and Comm. Engr. of Japan, Tokyo, Japan, 1975.
19. H. Kanbe, T. Kimura, and Y. Mizushima, IEEE Trans. Electron Dev., *ED-24* (1977), p. 713.
20. T. E. Seidel, D. E. Iglesias, and W. C. Niehaus, IEEE Trans. Electron Dev., *ED-21* (1974), p. 523.
21. R. J. McIntyre, IEEE Trans. Electron Dev., *ED-19* (1972), p. 703.
22. R. J. McIntyre, IEEE Trans. Electron Dev., *ED-20* (1973), p. 637.
23. A. S. Grove, *Physics and Technology of Semiconductor Devices,* New York: John Wiley, 1967, p. 176.